

# An experiment on magnetic induction pulses

José A. Manzanares

Depto. Termodinámica, Fac. de Física, Universidad de Valencia, 46100 Burjassot, Spain

Juan Bisquert, Germà Garcia-Belmonte, and Mercedes Fernández-Alonso

Dept. Ciències Experimentals, Campus de Borriol, Universitat Jaume I, 12080 Castelló, Spain

(Received 5 May 1993; accepted 7 March 1994)

The voltage pulse induced by a bar magnet as it moves at constant velocity through the axis of a circular coil is analyzed. The physical system considered has a number of interesting features: (a) It is easy to set up and handle in the laboratory, (b) the observed pulse can be predicted theoretically by means of a simple model, and (c) it provides a very vivid and direct illustration of the concept of electromagnetic induction. In fact, the system of a coil and magnet in relative motion is usually presented in textbooks when introducing this concept. The experiment can also be used as a procedure for determining the magnetic dipole moment of magnets. Since the equipment, a digital storage oscilloscope or computer, is usually available in undergraduate laboratories, the experiment can be performed in the introductory physics course.

## I. INTRODUCTION

We have studied the electromagnetic perturbation produced on a coil by a magnet moving through it. The resulting signal is obtained in the form of a plot of induced voltage vs time, which is recorded on a digital storage oscilloscope or computer. This curve can be used to determine the magnetic properties of the moving magnet.<sup>1-4</sup>

Similar induced voltage curves are often used in tutorial experiments to illustrate the effects of the time varying magnetic fluxes on closed circuits. Here, we will focus on a simple experiment in which the quantitative analysis of the pulse is simple. Indeed, our experiment is sufficiently straightforward that it can be employed as a laboratory experiment in the introductory physics course. The particular system we choose is a thin circular coil that is traversed by a bar magnet moving at constant speed along the axis of the coil.<sup>1,2</sup> Figure 1 shows a schematic diagram of the experimental setup. The main instrumentation needed is an air track with its usual accessories, a large diameter coil, an operational amplifier, and a digital storage oscilloscope. Alternatively, a computerized data acquisition system can be employed, which not only improves the experiment but also makes it more interesting for the students. The bar magnet is attached to a glider placed on the air track and launched towards the coil. As the magnet moves along the axis of the coil, the magnetic flux through the coil,  $\Phi_m$ , changes, and an electromotive force,  $\varepsilon = -d\Phi_m/dt$ , appears at the coil ends. We refer to the resulting curve  $\varepsilon(t)$  as the *induction pulse*.

The theoretical analysis employs a dipolar model for the magnet in which the magnetic field is approximated by the vector sum of the fields produced by a pair of magnetic point charges or monopoles.<sup>5</sup> This model can be handled by freshmen, and can be presented on a more rigorous basis for advanced students.<sup>6</sup> Alternatively, a solenoid model could also be employed, but this procedure requires the numerical computation of the magnetic field of the magnet by decomposing the solenoid into a large number of length elements and using the Biot-Savart law.<sup>4</sup> Fortunately, such a tedious procedure is not necessary when the cross section of the coil is much larger than that of the magnet.

Hence, the physical system considered has a number of interesting features: (a) It is easy to set up and handle in the laboratory, (b) the resulting curve can be theoretically pre-

dicted by means of a simple model, and (c) it provides a very vivid and direct illustration of the concept of electromagnetic induction. In fact, the system of a coil and magnet in relative motion is usually presented in textbooks when introducing this concept.<sup>7-9</sup>

## II. THEORETICAL MODEL

In order to work out a quantitative description of the induction pulse, we consider first the magnet model in detail. A homogeneously magnetized, long thin magnet can be regarded as composed of two fictitious magnetic charges of opposite sign placed at its ends. Thus two point charges or monopoles of magnitude  $q_m$  and opposite signs are placed at the ends of the magnet separated by a distance  $L$ . If  $m$  is the magnetic dipole moment of the magnet, these charges can be written as  $q_m^\pm = \pm m/L$ .

The magnetic field created by the positive pole  $q_m^+$  at a distance  $r$  is

$$B^+(r) = \frac{\mu_0 q_m^+}{4\pi r^2} \quad (1)$$

and points radially outwards. The emf in the coil induced by this pole as it moves along the axis of the coil is obtained, according to Faraday's law, as the time derivative of the magnetic flux through the coil. As is well known,<sup>10</sup> the flux through the coil due to the field in Eq. (1) can be calculated on any surface bounded by the coil. We choose the spherical segment of radius  $r = (x^2 + R^2)^{1/2}$  shown in Fig. 2, where  $x$  is the distance between the pole and the coil center and  $R$  is the coil radius. Since the magnetic field is normal to this surface at every point, the flux is given by the product

$$\Phi_m^+(x) = \text{sgn}(x) N B^+ S, \quad (2)$$

where  $N$  is the number of turns in the coil, and  $S$  is the area of the spherical segment,

$$S = 2\pi r(r - |x|). \quad (3)$$

Note that the sign of the magnetic flux is arbitrary but  $\Phi_m^+$  changes its sign when the pole passes through the coil. Here  $\Phi_m^+$  is taken to be negative when  $x < 0$ , and hence Eq. (2) incorporates as a factor the sign of  $x$ , i.e.,  $\text{sgn}(x)$ . From Eqs. (1)–(3), the flux is

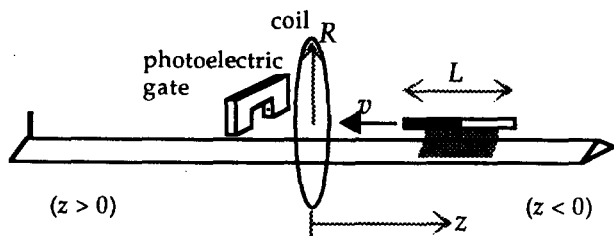


Fig. 1. Sketch of the experimental setup.

$$\Phi_m^+(x) = \text{sgn}(x) \frac{N\mu_0 q_m^+}{2} \left[ 1 - \frac{|x|}{(x^2 + R^2)^{1/2}} \right]. \quad (4)$$

Finally, the emf induced in the coil by the pole can be written as

$$\begin{aligned} \varepsilon^+(x) &= -\frac{d\Phi_m^+}{dt} = -\frac{dx}{dt} \frac{d\Phi_m^+}{dx} = -v \frac{d\Phi_m^+}{dx} \\ &= \frac{vN\mu_0 q_m^+ R^2}{2(x^2 + R^2)^{3/2}} \quad (x \neq 0), \end{aligned} \quad (5)$$

where  $v$  is the velocity of the pole. The condition on  $x$  in Eq. (5) comes from the fact that  $\Phi_m^+(x)$  is discontinuous at  $x=0$ . The induced emf, however, is continuous at  $x=0$ , though it cannot be obtained there as a time derivative of the magnetic flux. (Note that the limits of  $d\Phi_m^+/dx$  when  $x \rightarrow 0^-$  and  $x \rightarrow 0^+$  coincide).

The expressions in Eqs. (4) and (5) may appear “unphysical,” because magnetic poles always appear in pairs. Consider now that  $z$  represents the distance between the center of the magnet and the center of the coil (see Fig. 1). Then, the distance from the coil to the front end of the moving magnet is  $z+L/2$ , and the distance from the coil to the rear end is  $z-L/2$ . (Remember that the magnet is launched towards the coil from the region of negative  $z$ .) By adding up two expressions such as that of Eq. (4) we can readily obtain the flux produced by the magnet.

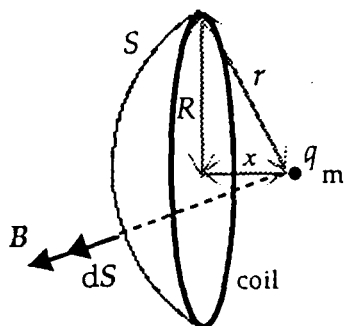


Fig. 2. Geometrical construction for the evaluation of the flux through the coil of the magnetic field created by a magnetic charge  $q_m$ . The spherical surface  $S$  is centered at the charge and lies on the coil.

$$\Phi_m(z) = \Phi_m^+(z+L/2) + \Phi_m^-(z-L/2)$$

$$\begin{aligned} &= \text{sgn}(z+L/2) \frac{N\mu_0 q_m^+}{2} \left\{ 1 - \frac{|z+L/2|}{[(z+L/2)^2 + R^2]^{1/2}} \right\} \\ &+ \text{sgn}(z-L/2) \frac{N\mu_0 q_m^-}{2} \left\{ 1 - \frac{|z-L/2|}{[(z-L/2)^2 + R^2]^{1/2}} \right\}. \end{aligned} \quad (6)$$

The emf induced by the magnet can now be written as

$$\begin{aligned} \varepsilon(z) &= \frac{vN\mu_0 m R^2}{2L} \left\{ \frac{1}{[(z+L/2)^2 + R^2]^{3/2}} \right. \\ &\quad \left. - \frac{1}{[(z-L/2)^2 + R^2]^{3/2}} \right\}. \end{aligned} \quad (7)$$

Equation (7) corresponds to the situation where the positive pole is leading the motion through the coil (see Eq. (6)).

In order to get  $\varepsilon$  as a function of time, we use  $z = v(t-t_0)$  where  $t_0$  is the time at which the center of the magnet is at the center of the coil. Rewriting Eq. (7) we find that

$$\begin{aligned} \varepsilon(t) &= \frac{vN\mu_0 m R^2}{2L} \left\{ \frac{1}{[(v(t-t_0)+L/2)^2 + R^2]^{3/2}} \right. \\ &\quad \left. - \frac{1}{[(v(t-t_0)-L/2)^2 + R^2]^{3/2}} \right\}. \end{aligned} \quad (8)$$

Equation (8) represents the induction pulse for a given magnet and coil with known values of  $v$  and  $t_0$ .

### III. EXPERIMENTAL

The diameter of the cylindrical magnet (PASCO SE-8604) is  $D = (1.000 \pm 0.005)$  cm and its length  $L = (5.015 \pm 0.005)$  cm. The coil (PHYWE 06 960.00) has  $N = 154$  turns, a radius  $R = (20.0 \pm 0.9)$  cm, and a thickness  $T = (1.7 \pm 0.1)$  cm. It is important to note that the magnet can be considered as an ideal “linear dipole” in the sense that its cross section is much smaller than the circular section bounded by the coil, and its length is much greater than its radius. Also, the coil can be considered as “infinitely thin” since its thickness is much smaller than its radius.

The velocity of the magnet is computed as  $v = L_{\text{eff}}/t_i$ , where  $t_i$  is the interruption time recorded by a photogate located near the coil and  $L_{\text{eff}}$  is the distance the magnet travels during the interruption time. Note that  $v$  is taken to be positive since the origin  $z=0$  is located at the coil center and the initial position of the glider corresponds to a negative value of  $z$  (see Fig. 1). Typically  $L_{\text{eff}}$  differs from the magnet length  $L$  by 1–2 mm; in the case of PHYWE gates  $L_{\text{eff}}$  is greater than  $L$ , but the opposite may occur with other gates.<sup>11</sup> Since  $L$  is about 5 cm, a rough determination of the magnet velocity as  $v = L/t_i$  would yield an error of a few percent, and consequently a lack of agreement between theory and experiment. Therefore, it is necessary to carefully determine  $L_{\text{eff}}$ . Methods for such a purpose have been considered in Ref. 11. Here we use two photogates along the air track which are separated by a distance  $D = 80$  cm. If the gates are connected so that the travel time  $T$  between them is recorded,  $L_{\text{eff}}$  can be obtained as

$$L_{\text{eff}} = \frac{Dt_i}{T}. \quad (9)$$

This procedure was repeated for magnet velocities ranging from 0.5 to 1.5 m/s, and the final average value was  $L_{\text{eff}} = (5.20 \pm 0.09)$  cm.

Further, when using Eq. (9), special care must be taken on a series of points: (i) the magnet must always cut the light beams at the same distance from the gate detector (e.g., the beam halfway), (ii) both gates must give the same reading for the interruption time (thus ensuring the constant velocity of the magnet), and (iii) the launcher must provide reproducible velocities (so that we can assume that the value of  $t_i$  can be obtained in a previous determination using the same position of the launcher).

The signal from the coil is first filtered and amplified, and the output is recorded on a digital scope or a computer with a data acquisition card. For this purpose, a noninverting voltage amplifier with amplification gain  $g = (121 \pm 2)$  and offset voltage  $V_{\text{offset}} = -(55 \pm 2)$  mV is used. The input impedance of this device is high enough (above 2 M $\Omega$ ) so that no current flows between the input terminals. Spurious signals, such as the local electrical network emission (50 Hz), are reduced by means of a filter which attenuates above 2 Hz. Since the characteristic frequency of the induction pulses is of the order of 1 Hz and the attenuation factor is less than 1% for frequencies below 2 Hz, no significant distortion caused by the filter is expected.

The sign of the signal depends on how the coil is connected to the digital scope or computer. According to the convention established in the previous section, we assume that a magnet whose positive pole is leading the motion induces a positive emf when approaching to the coil. Note that the direction of the induced current and the polarity of the emf in the coil are physically determined by Lenz's law.

The dipole moment  $m$  of the magnet deserves special attention, since it is the only parameter in our model which is not available from a direct measurement. The magnetic dipole moment was determined by two independent procedures. In the first method, the magnet is hung at its midpoint so that it can oscillate in a known, constant magnetic field created by a pair of Helmholtz coils.<sup>12</sup> The frequency of the small oscillations is measured for different intensities of the field, and a representation of the oscillation frequency squared versus the magnetic field yields a straight line of slope proportional to  $m$ . The second method<sup>13</sup> is based on the theoretical expression of the magnetic field along the magnet axis at a distance  $z$  from its center. From Eq. (1) this field is given by

$$B_{\text{th}}(z) = \frac{\mu_0 m}{4\pi L} \left[ \frac{1}{(z - L/2)^2} - \frac{1}{(z + L/2)^2} \right]. \quad (10)$$

The magnetic field  $B_{\text{ex}}$  is measured by means of a Hall probe (PHYWE 11 749.01) placed at a set of equidistant points from  $z = 8.5$  to 17.5 cm. A plot of  $B_{\text{ex}}$  vs the theoretical values of  $B_{\text{ex}}/m$  at the same points also yields a straight line of slope  $m$ . In our case, both determinations of the magnetic dipole moment agree within the experimental uncertainty, and the mean value is  $m = (2.055 \pm 0.015)$  A m<sup>2</sup>. It is interesting to note that Eq. (10) contains the length of the magnet (i.e., the magnet is modeled as a finite-length dipole) and that the magnetic field is measured at points which are far enough from the end of the magnet. A significant error in the determination of the magnetic dipole moment would have been obtained otherwise.<sup>4,13</sup>

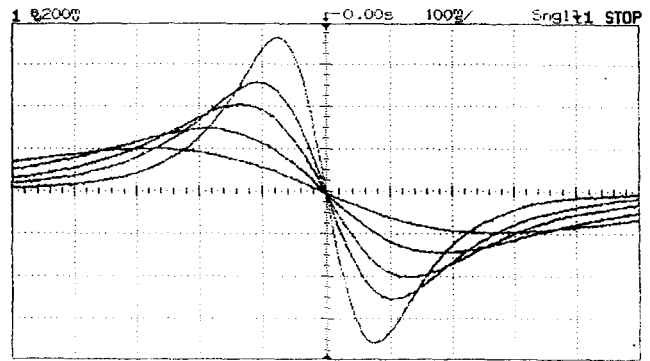


Fig. 3. Induction pulses in the digital oscilloscope corresponding to different magnet velocities. This record was obtained by using the autostore display mode, which allows for keeping the previous records on the same screen. The signals have been previously filtered and amplified with a gain of the order of one hundred. The trigger conditions were (i) level at zero volts, and (ii) negative slope.

#### IV. RESULTS

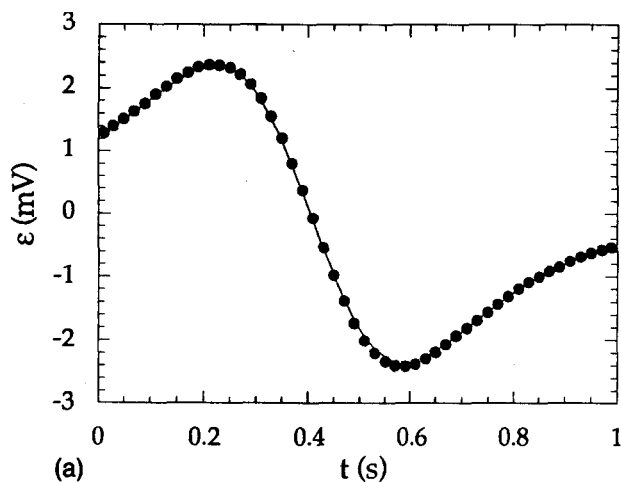
Figure 3 shows the printout of several induction pulses recorded in a HP 54600A digital scope when the magnet was launched towards the coil with different velocities. This figure has been obtained by using the *autostore* display mode of the scope (which allows for keeping the previous records), and setting the trigger level at  $\varepsilon = 0$ , so that the midpoint of the display corresponds to the instant  $t_0$  for all these curves.

In order to compare Eq. (8) with experiment, we also record the pulse on a Macintosh LC II computer with a data acquisition card and appropriate software (LABVIEW 2, National Instruments Inc.). The interruption time  $t_i$  of the gate can also be recorded by the computer by connecting the analog output of the gate to another input channel of the card. Data from the coil and the gate are acquired during 1 s at 1 kHz. The data acquisition frequency and the precision of the gate determine that the error in the recorded value for  $t_i$  is of the order of 1 ms. Then, there is no need to run the data acquisition system at a higher frequency—this would only delay the data analysis.

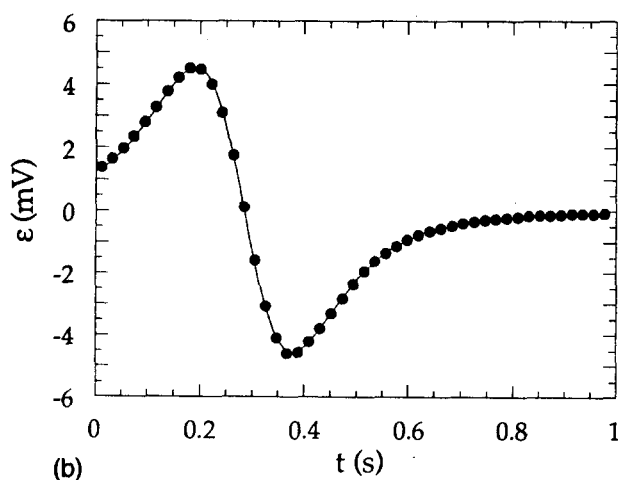
The only parameter in Eq. (8) that remains to be determined is the time  $t_0$ . Since this time satisfies the condition  $\varepsilon(t_0) = 0$ , it can be obtained from a linear plot of the experimental points near  $\varepsilon = 0$ . Finally, the computer is ready to compare the theoretical pulse corresponding to the experimental pulse, as shown in Figs. 4. The agreement is excellent and the results are very reproducible.

Let us analyze Figs. 3 and 4 and consider the dependence of  $\varepsilon(t)$  on the velocity  $v$  of the magnet. Equations (5) and (7) predict that the induced emf should be proportional to  $v$ . Figure 5 shows that this is indeed the case. The values of  $\varepsilon(t)$  at the peaks are plotted against  $v$  in this figure and a linear dependence with slope 4.19 mV s m<sup>-1</sup> is observed; a zero intercept at the origin has been imposed.

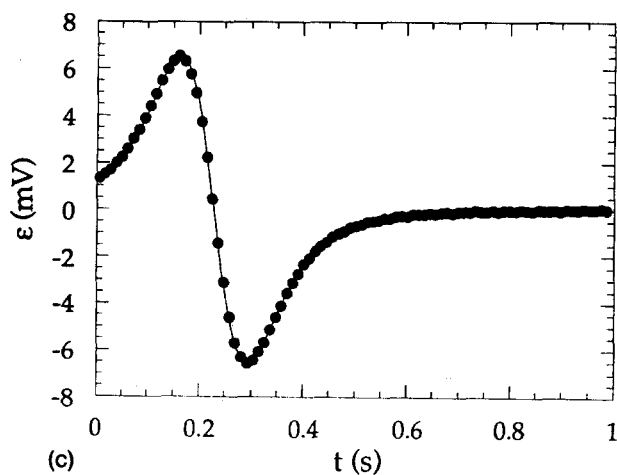
Figures 3 and 4 suggest that the area of the “half” pulse is velocity independent. When the magnet velocity decreases, the height of the peak decreases and the pulse widens, and this area seems to remain constant. We can easily show that this is indeed the case. Let  $t_0$  be the time instant when the magnet center and the coil center are coincident ( $z = 0$ ), and



(a)



(b)



(c)

Fig. 4. Induction pulses in the computer screen corresponding to different magnet velocities: (a) 0.56 m/s, (b) 1.08 m/s, and (c) 1.56 m/s. The circular spots are experimental values recorded by the computer and the continuous lines correspond to Eq. (8). The effects of the amplification (gain and offset) have been removed, so that the values in this plot represent the actual emf at the coil ends.

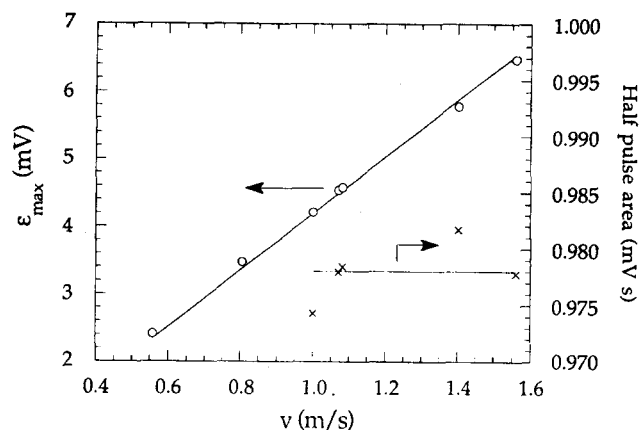


Fig. 5. Peak value of the induction pulse and absolute value of the "late half pulse" area corresponding to different magnet velocities.

$t_0^-$  the time instant when the positive pole of the magnet is at the coil center ( $z=L/2$ ). The area of the "late half pulse" can be expressed as

$$\int_{t_0}^{\infty} \varepsilon dt = - \int_{t_0}^{\infty} \frac{d\Phi_m}{dt} dt - \int_{t_0}^{t_0^-} \frac{d\Phi_m}{dt} dt$$

$$= \Phi_m(t_0) + \Delta\Phi_m^-(t_0^-), \quad (11)$$

where  $\Delta\Phi_m^-(t_0^-)$  is the jump in  $\Phi_m^-$  when the negative pole passes through the coil. [Note that the integral in the left-hand side of Eq. (11) has to be split in two because of the discontinuity of  $\Phi_m = \Phi_m^+ + \Phi_m^-$  at  $t_0^-$ .] In Eq. (11), we have used the fact that the flux is zero when  $t \rightarrow \infty$ . Since  $\Phi_m(t_0) = \Phi_m(z=0)$  can be obtained from Eq. (6) as

$$\Phi_m(t_0) = \frac{N\mu_0 m}{L} \left\{ 1 - \frac{L/2}{[(L/2)^2 + R^2]^{1/2}} \right\}, \quad (12)$$

and from Eq. (4)

$$\Delta\Phi_m^-(t_0^-) = -\Delta\Phi_m^+(t_0^+) = -\frac{N\mu_0 m}{L}, \quad (13)$$

we finally have

$$\int_{t_0}^{\infty} \varepsilon dt = -\frac{N\mu_0 m}{(L^2 + 4R^2)^{1/2}}. \quad (14)$$

Figure 5 shows that this area is indeed constant with velocity within the experimental error.

It is also interesting to consider the effect of the magnetic dipole moment  $m$  of the magnet on the pulse. Equations (7) and (8) show that the induced emf, just like the magnetic field created by the magnet, is proportional to  $m$ . Similar arguments to those considered before when discussing the dependence of the pulse on  $v$  indicate that both the peak value of  $\varepsilon(t)$  and the area of the half pulse should be proportional to the dipole moment of the magnet. This suggests that the value of  $m$  could be determined from the induction pulses obtained by launching the magnet with different velocities. Indeed, by using Eq. (14) and the average area of the "late half pulse" shown in Fig. 5 (i.e., 0.978 mV s) we can obtain the value  $m = (2.04 \pm 0.02) \text{ A m}^2$  for the dipole mo-

ment of the magnet, which is in agreement with the result  $m=(2.05\pm0.02)\text{ A m}^2$  obtained by using the Hall probe, as described in the experimental section.

## V. SUMMARY

Our simple model provides reasonable explanations for the observed phenomena. Further improvements, like the finite thickness of the coil, could be easily introduced in the model but this is beyond the scope of the simple analysis attempted here.

The system can also be used to determine the dipole moment of the magnet. This can be done either by calculating the area of the half pulse as described in the previous section or by using a computer routine for multiparametric nonlinear fitting. In the second case, the fitting equation given to the computer is Eq. (8), with  $m$  and  $t_0$  as free parameters. (Letting  $t_0$  be undetermined is convenient though not necessary.) This procedure has a high degree of reproducibility (dispersion lower than 1%), and the results agree, within the experimental error, with the previous determinations of  $m$ . Moreover, the dispersion of  $m$  can be obtained by launching the glider through the coil at different velocities.

## ACKNOWLEDGMENTS

We would like to thank Salvador Mafé for his valuable contributions, and José Manuel Claver for his assistance in the design of the data acquisition system.

- <sup>1</sup>L. Basano, P. Ottonello, and C. Pontiggia, "The magnet-solenoid equivalence: A modern experiment using a personal computer," *Am. J. Phys.* **56**, 517–521 (1988).
- <sup>2</sup>Lanny J. Reed, "Magnetic induction and the linear air track," *Am. J. Phys.* **43**, 555–556 (1975).
- <sup>3</sup>Jhules A. M. Clack and Terrence P. Toepker, "Magnetic induction experiment," *The Physics Teacher*, April, 236–238 (1990).
- <sup>4</sup>Cyrus S. MacLachy, Philip Backman, and Larry Bogan, "A quantitative magnetic braking experiment," *Am. J. Phys.* **61**, 1096–1101 (1993).
- <sup>5</sup>Marcel Wellner, *Elements of Physics* (Plenum, New York, 1991), p. 395.
- <sup>6</sup>Arnold Sommerfeld, *Electrodynamics* (Academic, New York, 1964), pp. 81–3.
- <sup>7</sup>David Halliday, Robert Resnick, and Jearl Walker, *Fundamentals of Physics*, 4th ed. (Wiley, New York, 1993), pp. 874–5.
- <sup>8</sup>Paul A. Tipler, *Physics for Scientists and Engineers*, 3rd ed. (Worth, New York, 1991), p. 841.
- <sup>9</sup>Raymond A. Serway, *Physics for Scientists & Engineers*, 3rd ed., revised (Saunders College, Philadelphia, 1992), pp. 882–3.
- <sup>10</sup>Reference 5, p. 88.
- <sup>11</sup>E. P. Mosca and J. P. Ertel, "Photogates: An instrument evaluation," *Am. J. Phys.* **57**, 840–844 (1989).
- <sup>12</sup>Reference 7, p. 922.
- <sup>13</sup>Juan Bisquert, Emilia Hurtado, Salvador Mafé, and José Pina, "Oscillations of a dipole in a magnetic field: An experiment," *Am. J. Phys.* **58**, 838–843 (1990); *ibid.* **59**, 567(E) (1991).

## Classical analogy to quantum mechanical level repulsion

Winfried Frank<sup>a)</sup> and Peter von Brentano  
*Institut für Kernphysik, Universität zu Köln, D-50937 Köln, Germany*

(Received 26 July 1993; accepted 8 February 1994)

The frequency repulsion in coupled harmonic oscillators can be treated as a classical analogy to the quantum mechanical level repulsion. As an example the inductively coupled LC circuit will be discussed.

### I. QUANTUM MECHANICAL TWO-LEVEL SYSTEM

The quantum mechanical two-level system is well known and has many applications in physics.<sup>1–3</sup> An example is the parity doublet spectrum of the  $\text{NH}_3$  molecule.<sup>3,4</sup> A very important property of two-state systems is level repulsion. Let the two-state system with no interaction have the energies  $E_1$  and  $E_2$ . The interaction should then be described by an off-diagonal symmetric and, for simplicity, real matrix with the matrix elements  $V_{12}$ ,  $V_{21}=V_{12}$ , and  $V_{11}=V_{22}=0$ . The Hamiltonian in matrix representation takes the form

$$H_{ik}=E_i\delta_{ik}+V_{ik} \quad \text{with } i,k=1,2. \quad (1)$$

The energies of the coupled system are

$$\bar{E}_{1,2}=\frac{1}{2}(E_1+E_2)\pm\frac{1}{2}\sqrt{(E_1-E_2)^2+4V_{12}^2}. \quad (2)$$

With this formula one can find the quantum mechanical level repulsion theorem

$$|\bar{E}_1-\bar{E}_2|\geq|E_1-E_2|. \quad (3)$$

This means the energy difference of two mixed states is always greater than or equal to the energy difference of two unmixed states. One may ask whether there are classical analogies to this level repulsion. In the following we shall see that coupled harmonic oscillators have this property and as an example we discuss the inductively coupled LC circuit. The calculations are elementary and in this sense are not really new. Our point is to emphasize the analogy between classical and quantum mechanical level repulsion and to illustrate this with a simple classical system.

### II. COUPLED HARMONIC OSCILLATORS

A frequency repulsion theorem can be established for two harmonic oscillators where one finds that the absolute difference of the eigenfrequencies increases if coupling between these oscillators is present.